

Risedronate Reduces Intracortical Porosity in Women With Osteoporosis

Babul Borah,¹ Tom Dufresne,¹ Joe Nurre,¹ Roger Phipps,^{1,2} Paula Chmielewski,¹ Leigh Wagner,¹ Mark Lundy,¹ Mary Bouxsein,³ Roger Zebaze,⁴ and Ego Seeman⁴

¹New Drug Development, Procter & Gamble Pharmaceuticals, Mason, OH, USA

²Maine Institute for Human Genetics and Health, Brewer, ME, USA

³Ortho Biomechanics Laboratory, Harvard Medical School, Boston, MA, USA

⁴Austin Health, University of Melbourne, Australia

ABSTRACT

Nonvertebral fractures account for 80% of all fractures and their accompanying morbidity and mortality. Despite this, the effect of drug therapy on cortical morphology has received limited attention, partly because cortical bone is believed to remodel less and decrease less with age than trabecular bone. However, the haversian canals traversing the cortex provide a surface for remodeling that produces bone loss, porosity, and cortical fragility. We developed a new method of 3D micro-computed tomography (μ CT) to quantify intracortical porosity and the effects of treatment. Women with osteoporosis randomized to risedronate (5 mg/day, $n = 28$) or placebo ($n = 21$) had paired transiliac biopsies at baseline and 5 years imaged using 3D μ CT. Pores determined from 8 to 12 slices were stratified by their minor axis length into those 25 to 100 μ m (closing cone of haversian canals), 100 to 300 μ m (cutting cone of haversian canals), and >300 μ m (coalescent cavities). Porosity was analyzed as pore area (percent bone area) and pore density (pore number/mm²). Medians are reported. Risedronate reduced pore area in the 25 to 100, 100 to 300, and 300 to 500 μ m ranges over 5 years ($p = .0008$, .04, NS, respectively) corresponding to an 18% to 25% reduction. In the placebo group, pore area was unchanged. At 5 years, pore area and pore number/mm² in the 25 to 100 μ m range were each 17% lower in the risedronate group than in the placebo group ($p = .02$ and .04, respectively). Risedronate is likely to maintain bone strength and reduce nonvertebral fracture risk in part by reducing remodeling and therefore the number and size of intracortical cavities. © 2010 American Society for Bone and Mineral Research.

KEY WORDS: CORTICAL POROSITY; HAVERSIAN CANALS; OSTEOPOROSIS; 3D MICRO-COMPUTED TOMOGRAPHY; RISEDRONATE

Introduction

Research efforts in preventing fractures have focused on the pathogenesis of accelerated trabecular bone loss and vertebral fragility in postmenopausal women.⁽¹⁻⁴⁾ However, 80% of all fractures and 80% of all the accompanying morbidity, mortality, and health costs in the community are the result of nonvertebral fractures.⁽⁵⁾ Moreover, these fractures occur at sites that are 70% to 80% cortical bone, which is believed to be lost more slowly than trabecular bone during advancing age because it is remodeled more slowly.⁽¹⁻⁴⁾

Recent evidence suggests that several of these notions need reappraisal.⁽⁶⁾ Remodeling requires a surface to occur upon.^(7,8) Although trabecular bone is fashioned with more surface per unit volume than cortical bone, haversian canals traversing the cortex provide a large intracortical surface area, exposing cortical bone to the high remodeling after menopause in women and

late in life in both sexes due to secondary hyperparathyroidism. For example, Han et al.⁽⁸⁾ reported higher remodeling intensity on the intracortical than on trabecular or endocortical surfaces. More recently, Zebaze et al.⁽⁶⁾ reported that most of the bone lost with age from the distal radius was intracortical not trabecular in origin.

Given the role of cortical bone in bone strength, the predominantly cortical composition of the appendicular skeleton, the common occurrence of nonvertebral fractures, and the lack of information concerning the effects of drug therapy on cortical morphology, we developed a new method of high-resolution micro-computed tomography (μ CT) to reconstruct and visualize the 3D longitudinal intersecting haversian canals within the iliac crest cortex that are seen as "porosity" in 2D histomorphometric images. We quantified the morphology of porosity according to pore size and number and determined whether 5 years of treatment with risedronate reduced

Submitted for publication on 19 January 2009. Accepted in revised form on 24 April 2009. Published ahead of print on 6 July 2009.

Address correspondence to: Babul Borah, Procter & Gamble Pharmaceuticals, MBC SB3-3J8, 8700 Mason Montgomery Road, Mason, OH 45040, USA.

E-mail: babul.borah@wcrx.com

Journal of Bone and Mineral Research, Vol. 25, No. 1, January 2010, pp 41-47

DOI: 10.1359/jbmr.090711

© 2010 American Society for Bone and Mineral Research

intracortical porosity in postmenopausal women with osteoporosis.

Materials and Methods

Postmenopausal women in the Vertebral Efficacy with Risedronate Therapy North American (VERT NA) trial with either two vertebral fractures at baseline or one prevalent vertebral fracture and a lumbar spine bone mineral density (BMD) *T*-score of -2 or less received daily risedronate 5 mg or placebo for up to 5 years.⁽⁹⁾ All received 1000 mg/day elemental calcium carbonate and vitamin D if deficient at baseline (500 IU/day cholecalciferol). Transiliac bone biopsies were obtained at baseline and 3 and 5 years for histomorphometric analysis.^(10,11) The 5-year biopsy was taken from the same side as the baseline but at least 2 cm distant from the previous biopsy. Only subjects with a biopsy at baseline and 5 years were included (risedronate $n=28$ and placebo $n=21$) in the present study. To be included, the biopsy was required to have at least one evaluable cortex. When both cortices were present, analysis was performed on the thicker cortex. The biopsies were imaged using the Scanco μ CT40 with a resolution of 8 μ m. The 16-bit gray-level cortical images were segmented into bone and pores using a fixed threshold.

Conventional 2D histomorphometric measurement of porosity is associated with a high variance arising from sampling variations, intersection heterogeneity of pore size and number, and subjective separation of the corticomedullary junction.⁽¹²⁾ The 3D μ CT method addresses several sources of this variability. The intersection variability was reduced by averaging porosity for each biopsy over 8 to 12 digital μ CT slices, approximately 300 to 400 μ m apart, parallel to the original histologic cut face. Porosity measurement using a single slice as performed in conventional histomorphometry had a coefficient of variation of more than 40% and this was reduced to less than 5% when 8 to 12 slices, 300 to 400 μ m apart, were used.

In iliac crest biopsies, the demarcation between compact cortex and trabecular compartments is indistinct due to trabecularization of the cortex adjacent to the marrow cavity.^(7,12–15) Subjective separation of cortex and trabecular bone introduces variability, as illustrated in Fig. 1. Intracortical porosity may be 5% if “compact” cortex adjacent to the periosteum is chosen or may be greater than 20% if large cavities adjacent to the marrow are chosen. To avoid arbitrary demarcation between “compact” and trabecular bone, we quantified porosity as a continuous variable by cavity sizes and measured porosity for a defined range of pore sizes, which reduces variability (see Fig. 1). Initially, a boundary between the cortex and trabecular bone was arbitrarily defined on the endosteal surface of a slice to include the intracortical and endocortical regions. All pores within the boundary were identified using connected components analysis and fitted to an ellipse to determine their minor axis.⁽¹⁶⁾ Pores were stratified by their minor-axis length in multiples of 8 μ m (minimum pixel size) and partitioned into ranges of increasing pore size of approximately 100 μ m (increments of 12 pixels). Pores with a minor axis of less than approximately 25 μ m (area with 3 pixels, osteocyte lacunae) were excluded.⁽¹⁷⁾ Pores in the approximate range of 25 to 100 μ m approximate haversian canals in the closing cone,^(18–20) and pores in the range of 100 to 300 μ m were attributed to the cutting cone excavated during the resorptive phase of remodeling.^(7,21–23) Pores with minor axis of 300 μ m or higher were assumed to result from coalescent cutting cones of adjacent remodeling units.⁽²⁴⁾

Analyses were performed blinded to treatment group and were automated using Matlab scripts and standard Matlab imaging functions.⁽²⁵⁾ The area of a pore was the number of pixels contained within the pore multiplied by the area of a pixel with dimensions of $8 \times 8 \mu\text{m}^2$. The pore area and bone area of all selected slices were summed to provide a total pore and bone area, respectively, for the entire biopsy. Porosity was expressed as pore area/bone area (%) and pore density as pore number per unit bone area (number/ mm^2) stratified by pore size, defined as

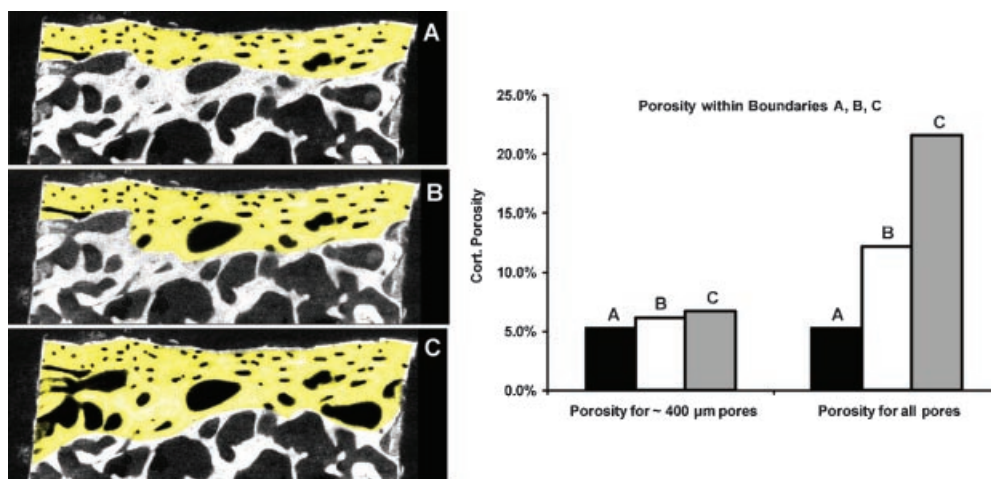


Fig. 1. (Left) Porosity is measured on a single μ CT slice with three different arbitrary boundaries shaded yellow in A, B, and C. (A) The boundary includes cavities close to the periosteum. (B) The boundary includes cavities in the periosteum and part of the endocortical envelope. (C) The boundary extends further into the endocortical zone and includes large trabecularized holes. (Right) When all pores within the boundary are included, porosity (%) gradually increases from $\sim 5\%$ (A) to $>20\%$ (C). When porosity is measured for a defined range of pores ($\sim 400 \mu\text{m}$ in this case), the variability is reduced. Although the absolute pore area and bone area changed, porosity at $\sim 6\%$ remained relatively unchanged within the three boundaries.

the minor ellipse axis lengths of 25 to 100, 100 to 300, 300 to 500, and 500 to 800 μm .

Statistical analysis was performed using SAS software (version 8.2, SAS Institute). Baseline characteristics were compared using one-way ANOVA. Nonparametric methods were used for within- and between-group comparisons because the Shapiro-Wilk test indicated that the data were not normally distributed. Therefore, medians are reported. For each pore-size range, the change and percentage change from baseline within and between groups were assessed using the Wilcoxon signed-rank test and the Wilcoxon rank-sum test, respectively.

Results

Pore morphology

Pores seen using histomorphometry and μCT are cross sections of longitudinally orientated haversian canals traversing the cortex (Figs. 2 and 3). Canals from adjacent osteons can coalesce at a point and then continue as separate canals (see Fig. 3). This diversity in cavity size, shape, and number is illustrated when four of the slices from a biopsy, 300 to 400 μm apart, are compared (Fig. 4). Depending on the cross section examined, porosity appeared as single isolated circular pore (slice 1), a dumbbell-shaped pore resulting from coalescence of two or more haversian canals (slice 2), or enlarged pores adjacent to the endocortical surface that can perforate it, producing trabecularization of cortical bone (slices 3 and 4).

Effects of treatment on porosity and pore density

The risedronate and placebo groups did not differ in baseline characteristics, including remodeling indices, pore area, and pore

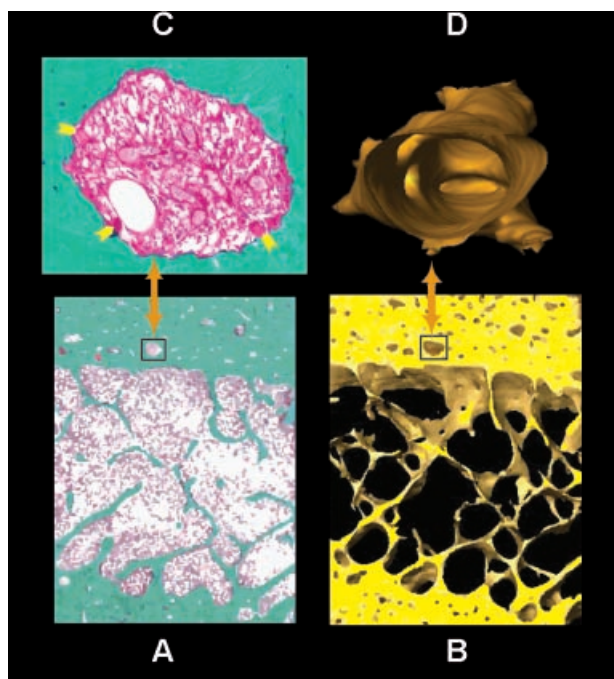


Fig. 2. (A) A 2D histologic section and (B) the corresponding 3D micro-computed tomography image. (C) A magnified view of a cutting cone with osteoclasts (arrows). (D) The corresponding 3D canal structure.

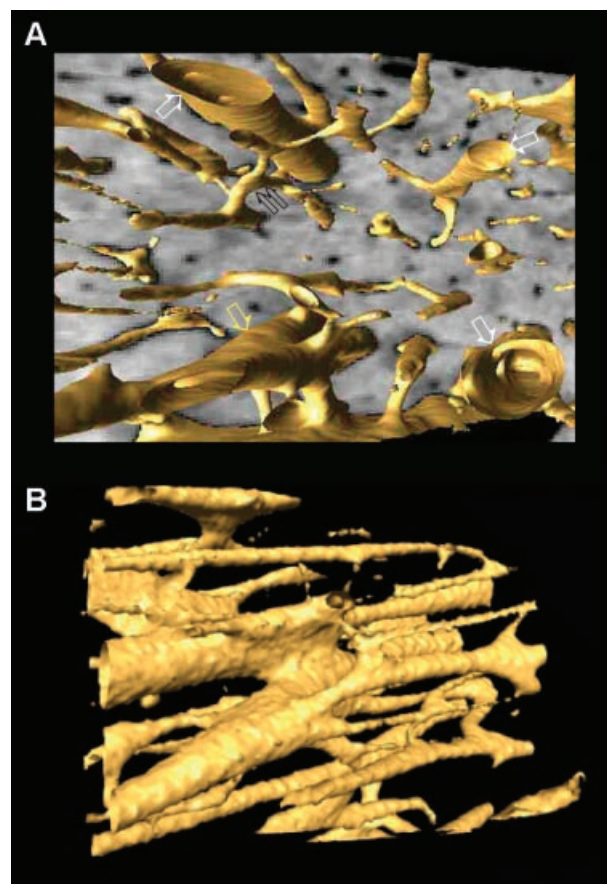


Fig. 3. (A) A 3D micro-computed tomography (μCT) image of the biopsy shows the haversian canals running perpendicular to the background of a 2D μCT section. Several large oval canals may reflect the cutting cone (open arrow). Volkmann canals are also shown (double arrow). (B) Canals from adjacent osteons coalesce at a point and then continue as two canals.

number (Tables 1 through 3). Median pore area/bone area in the 25 to 100, 100 to 300, and 300 to 500 μm ranges decreased in the risedronate group over 5 years ($p = .0008$ and 0.4 , NS, respectively) and remained unchanged in the placebo group (see Table 2). This corresponded to a reduction of 18% to 25% in the risedronate group and -0.3% to 1.3% in the placebo group (Fig. 5). Although these percentage changes between groups did not achieve statistical significance, at 5 years, the pore area/bone area was 17% lower in the risedronate than in the placebo group for pores in the 25 to 100 μm range ($p = .02$). Median pore number/ mm^2 decreased by 8% to 17% in the risedronate group and increased by 2% to 49% in the placebo group for the 25 to 100, 100 to 300, and 300 to 500 μm ranges. Although these changes were not significant between groups, the pore number/ mm^2 in the 25 to 100 μm range was 17% lower in the risedronate group than in the placebo group at 5 years ($p = .04$; see Table 3).

Discussion

Bone remodeling removes microdamage within the bone matrix deep to a surface.⁽²⁶⁾ The cells responsible for the removal of damage and restoration of bone arise from the marrow, the bone-lining cells, or the circulation and must reach the site of

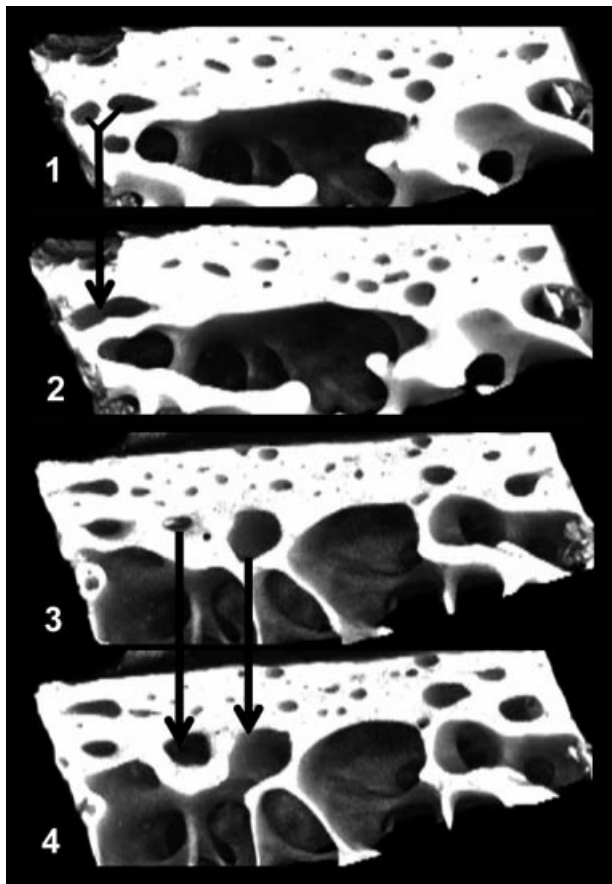


Fig. 4. Four adjacent slices 300 to 400 μm apart show interslice heterogeneity in pore size, shape, and number in the same biopsy. The arrows show the coalescence of two canals forming a dumbbell-shaped cavity (slices 1 and 2) and the transformation of a cavity (slice 3) into a larger cavity (slice 4).

Table 1. Demographic and Baseline Characteristics [Mean (\pm SD)]

	Risedronate, <i>N</i> = 28 (<i>n</i>)	Placebo, <i>N</i> = 21 (<i>n</i>)
Age, years	67.5 \pm 5.8 (28)	64.3 \pm 8.5 (21)
Lumbar spine BMD <i>T</i> -score	-2.5 \pm 1.1 (16)	-1.8 \pm 1.9 (16)
Femoral neck BMD <i>T</i> -score	-2.0 \pm 0.7 (28)	-1.7 \pm 1.0 (21)
Years since menopause	21.3 \pm 7.7 (28)	17.5 \pm 10.0 (21)
No. of prevalent vertebral fractures	2.0 \pm 1.5 (28)	1.7 \pm 1.8 (21)
Mineralizing surface/bone surface, %	6.4 \pm 4.1 (23)	7.6 \pm 6.3 (15)
Activation frequency, no. per year	0.4 \pm 0.2 (20)	0.4 \pm 0.3 (13)

N = number of patients within specified treatment; *n* = number of patients.

Baseline characteristics were not statistically different between groups (one-way ANOVA).

BMD, bone mineral density; SD, standard deviation.

damage deep within the matrix.⁽²⁷⁾ The lining cells of the trabecular, endocortical, and intracortical components of the endosteal or inner bone envelope form the conduit facilitating communication between the damaged matrix and the marrow environment. Remodeling is initiated on these surfaces, the linings of which form the roof of the remodeling compartment, within which excavation of old or damaged bone is followed by incomplete replacement with new bone.^(26,27)

Remodeling proceeds rapidly in trabecular bone because of its large surface/bone volume; because trabeculae are resorbed, their surfaces disappear, and so remodeling diminishes in the trabecular compartment. However, remodeling continues on the endocortical surface of the cortex adjacent to marrow and on the intracortical surface formed by the lining of haversian canals.⁽⁸⁾ Erosion of cortical bone, particularly adjacent to marrow, trabecularizes as adjacent resorptive cavities coalesce, producing giant canals of irregular shape and blurring the distinction between cortical and trabecular bone.^(6,7,13,24)

We avoided dichotomizing cortical and trabecular bone for this reason and analyzed porosity as a continuous variable by dividing the sizes of cavities according to the physiologic processes likely to be producing them. Porosity in the 25 to 100 μm range was likely to reflect haversian canals in the closing cone, 100 to 300 μm resorption sites excavating the cortex as a cutting cone, and larger cavities reflecting coalescent resorption cavities arising from haversian canal surfaces where a remodeling event arises. Cavities in the 25 to 100 and 100 to 300 μm ranges were equally prevalent throughout the cortex. Cavities larger than 300 μm were more abundant in the endocortical region (Fig. 6).

When risedronate is administered, pores excavated *before* treatment complete their remodeling cycle with bone formation *during* treatment, thereby reducing their size. Concurrently, the appearance of new remodeling units is suppressed by 70% to 80%, so the extent of the bone surface undergoing resorption decreases by about 50%.^(10,11) In controls, remodeling remains high, and some remodeling sites may colocalize, enlarging cavities before they have had the opportunity to undergo the filling phase of their remodeling cycle.

Peak stress at yield and torsional toughness decrease precipitously when porosity increases by a few percentage points.^(18,28-31) We observed an 18% to 25% decrease in pore area in the 25 to 100, 100 to 300, and 300 to 500 μm ranges over 5 years in the treated group, with no change or increases in porosity in the placebo group. Likewise, pore numbers decreased by 8% to 17% during treatment with risedronate but increased in the placebo group (see Fig. 5). Although change in porosity for larger pore sizes did not reach statistical significance, at 5 years, there were 17% fewer resorption cavities in the 25 to 100 μm range in the treated group compared with placebo across the cortical surface from periosteum to endosteum.

We propose that nonvertebral fracture risk reduction is only 20% to 30%, about half the vertebral fracture risk reduction achieved with most drugs, because the extent of architectural decay at nonvertebral (largely cortical) sites is severe by the time treatment is usually started (\sim 65 to 70 years).⁽³²⁾ Such late intervention may limit the efficacy of most treatments. Partial

Table 2. Porosity Expressed as the Pore Area/Bone Area (%) for Each Range of Cavity Sizes [Median (25th, 75th Interquartile Range)]

Pore size Minor axis length (μm)	Pore area/bone area (%) risedronate group (N = 28)			Pore area/bone area (%) placebo group (N = 21)		
	Baseline	5 years	Change (n)	Baseline	5 years	Change (n)
25–100	1.56 (1.31, 1.95)	1.33 ^a (1.0, 1.54)	-0.31 ^{b,c} (-0.70, 0.03) (p = .0008) (28)	1.77 (1.13, 2.18)	1.61 (1.29, 2.06)	-0.01 (-0.49, 0.39) (21)
100–300	3.73 (3.10, 5.58)	2.73 (2.18, 5.04)	-1.11 ^b (-1.90, 0.15) (p = .04) (28)	3.37 (2.49, 5.59)	3.45 (2.44, 4.81)	0.02 (-1.80, 1.41) (21)
300–500	2.44 (1.67, 3.65)	2.02 (1.04, 3.77)	-0.87 (-1.69, 1.33) (25)	2.10 (0.88, 2.97)	2.34 (1.15, 3.29)	0.01 (-0.71, 1.81) (21)
500–800	2.74 (1.64, 4.22)	4.48 (1.04, 9.25)	1.0 (-1.39, 6.40) (17)	1.81 (1.11, 3.56)	3.45 (1.96, 4.30)	1.24 (-0.84, 2.44) (12)

^aLower than placebo, p = .02, Wilcoxon rank-sum test.

^bReduction from baseline, p ≤ .05, Wilcoxon signed-rank test.

^cReduction with risedronate greater versus placebo (p = 0.08, Wilcoxon rank-sum test).

N = number of patients; n = number of actual paired biopsies analyzed.

Table 3. Porosity Expressed as the Number of Pores/mm² for Each Range of Cavity Sizes [Median (25th, 75th Interquartile Range)]

Pore size Minor axis length (μm)	No. of pores per mm ² risedronate group (N = 28)			No. of pores per mm ² placebo group (N = 21)		
	Baseline	5 years	Change (n)	Baseline	5 years	Change (n)
25–100	3.23 ^a (2.64, 3.71)	2.83 ^b (2.52, 3.51)	-0.37 (-1.28, 0.44) (28)	2.90 (2.34, 4.20)	3.41 (2.95, 3.92)	0.06 (-0.68, 0.84) (21)
100–300	0.86 ^a (0.51, 1.17)	0.69 (0.51, 1.04)	-0.17 (-0.49, 0.26) (28)	0.75 (0.36, 1.07)	0.72 (0.45, 1.09)	0.02 (-0.60, 0.36) (21)
300–500	0.11 ^a (0.07, 0.19)	0.10 (0.06, 0.15)	-0.01 (-0.06, 0.05) (25)	0.07 (0.04, 0.14)	0.11 (0.07, 0.18)	0.03 (-0.01, 0.09) (21)
500–800	0.06 ^a (.03, 0.08)	0.08 (0.03, 0.15)	0.10 (-0.02, 0.10) (17)	0.04 (0.02, 0.06)	0.06 (0.05, 0.09)	0.01 (0.01, 0.05) (12)

^aNot significantly different from placebo at baseline.

^bp = .04 versus placebo at 5 years, Wilcoxon rank-sum test.

N = number of patients; n = number of actual paired biopsies analyzed.

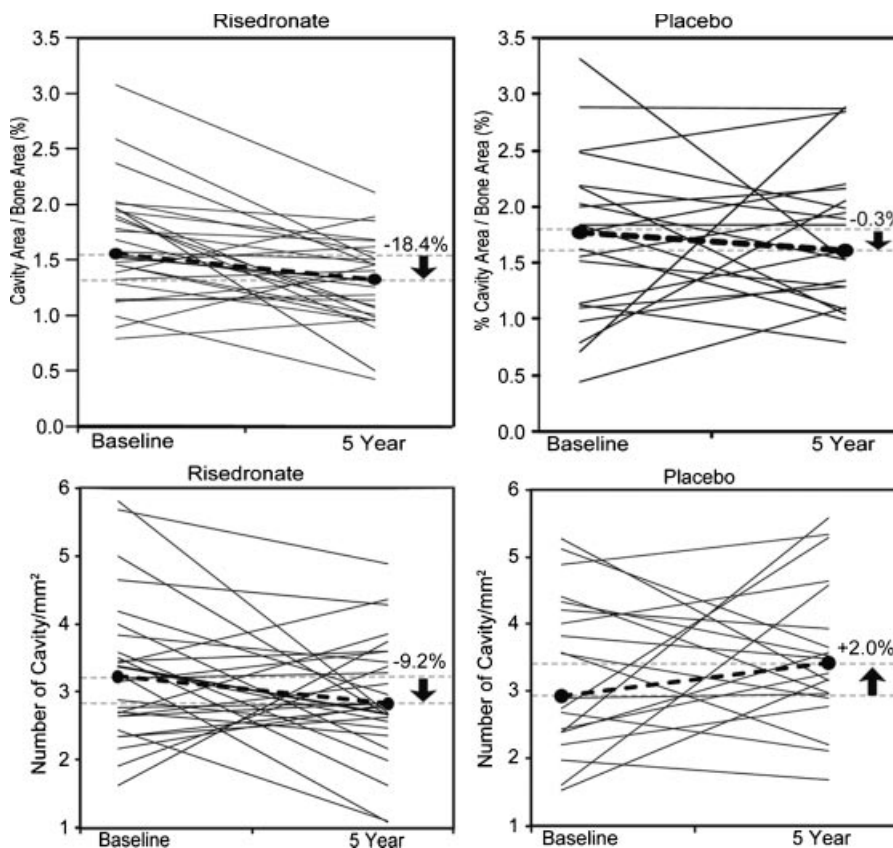


Fig. 5. Changes in pore area/bone area (%) and pore density (pore number/mm²) for the 25 to 100 μm range between baseline and 5 years in each subject in the risedronate and placebo groups. The magnitude and direction of the median percentage changes are shown.

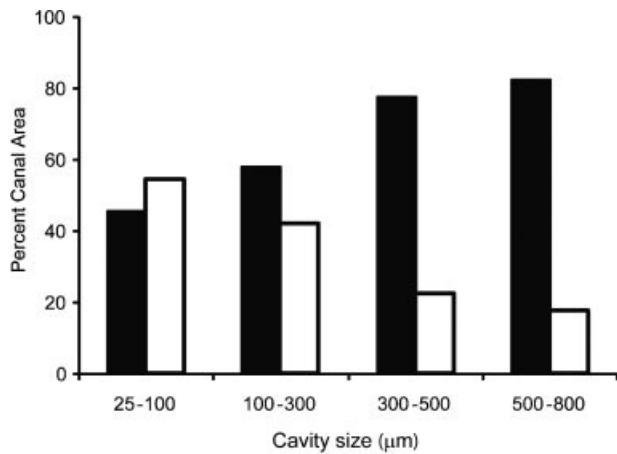


Fig. 6. Distribution of pore sizes in the endosteal (*black bars*) and periosteal (*open bars*) regions of the cortex according to their size. The pores with minor axis of 300 μm or less are equally prevalent throughout the cortex. Pores greater than 300 μm are more abundant in the endocortical region.

filling of large coalescent pores is unlikely to modify pore area in a biologically meaningful way because the area produced by multiple overlapping pores is too large to be refilled by bone formation, which is reduced by 30% to 40% in the elderly.^(33–36) Antiresorptive agents such as risedronate reduce resorption mainly by reducing the birth rate of basic multicellular units. Prevention of bone loss and structural decay also may occur by reducing the volume of bone resorbed or increasing the volume of bone deposited by each of the fewer basic multicellular units still remodeling bone, but evidence for either mechanism is lacking.

A limitation of this study is the sample size and the heterogeneity in porosity from slice to slice. The extent of porosity defined as pore area (percent bone area) was 1.6% to 4%, and pore number was 0.1 to 3.2/ mm^2 before treatment. These small quantities change by small increments; reductions produced by risedronate in pore area ranged from 18% to 25%, whereas for placebo, reductions ranged from -0.3% to 1.3%. Also, reductions produced by risedronate in pore number ranged from 8% to 17%, whereas for placebo it increased from 2% to 49%. These factors limited our ability to observe changes with statistical significance, at least for the larger (and fewer) pores. To achieve statistical significance in the observed median difference in cortical porosity of 18% or higher, a study with 50 or more paired biopsies from patients per treatment group would be required. Nevertheless, we were able to detect changes in pores of smaller dimensions consistent with our current understanding of the pathogenesis of porosity and the effects of antiresorptives on bone remodeling. Cortical bone was assessed at the iliac crest; whether findings at other regions would be similar is not known. However, the reduction of remodeling of the iliac crest has been shown to be consistent with the antifracture efficacy of risedronate.^(10,11)

In summary, cortical bone is traversed by haversian canals, which provide a surface for remodeling. Increasing cortical porosity and cortical thinning weaken the bone. Risedronate suppresses bone remodeling and, therefore, reduces the

appearance of new cortical pores, as reflected in fewer pores after 5 years, compared with controls. The surface area of smaller pores also was reduced as the bone-formation phase of remodeling went to completion (rather than these cavities being enlarged by continued remodeling). In controls, pore area and pore number increase as high remodeling continues to erode the cortex. The reduced intracortical porosity with risedronate is likely to contribute to the slowing of progression and perhaps partial reversal of fragility, which reduces fracture risk.

Disclosures

B Borah, T Dufresne, J Nurre, P Chmielewski, L Wagner, and M Lundy are employees of Procter & Gamble Pharmaceuticals. R Phipps, who was an employee of P&GP during the study period, is no longer an employee but still owns stocks and stock options of P&GP. R Zebaze declares that he has no conflict of interest. E Seeman is an advisory committee member and speaker at national and international industry-sponsored symposia for Eli Lilly, Sanofi-Aventis, Procter & Gamble Pharmaceuticals, Servier, Amgen, Novartis, and Merck & Co. M Bouxsein served as consultant for Amgen, Merck & Co. and Acceleron Pharma.

Acknowledgments

The authors thank Diane Vonderheide in preparing the graphic artwork. We acknowledge the editorial support of Dr. Betty L Thompson (*Excerpta Medica*). We thank the Alliance for Better Bone Health (Procter & Gamble Pharmaceuticals and Sanofi-Aventis) for sponsoring this study. The interpretation of findings and conclusion in this article are those of the authors and do not necessarily represent the views of the sponsors.

References

- Albright F, Smith PH, Richardson AM. Postmenopausal osteoporosis. *JAMA*. 1941;116:2465–2474.
- Riggs BL, Wahner HW, Melton LJ, Richelson LS, Judd HL, Offord KP. Rates of bone loss in the appendicular and axial skeletons of women: evidence of substantial vertebral bone loss before menopause. *J Clin Invest*. 1986;77:1487–1491.
- Riggs BL, Melton LJ 3rd, Robb RA, et al. Population-based study of age and sex differences in bone volumetric density, size, geometry and structure at different skeletal sites. *J Bone Miner Res*. 2004;19:1945–1954
- Riggs BL, Melton LJ, Robb R, et al. A population-based assessment of rates of bone loss at multiple skeletal sites: evidence for substantial trabecular bone loss in young adult women and men. *J Bone Miner Res*. 2008;23:205–214.
- Kanis JA, Johnell O, Oden A, Dawson A, De Laet C, Jonsson B. Ten year probabilities of osteoporotic fractures according to BMD and diagnostic thresholds. *Osteoporos Int*. 2001;12:989–995.
- Zebaze R, Ghasem A, Bohte A, et al. The neglected role of intracortical remodeling in age-related bone loss. *J Bone Miner Res*. 2008;23:S29.
- Parfitt AM. Surface specific bone remodeling in health and disease. In: Kleerekoper M, Krane S, eds. *Clinical Disorders of Bone and Mineral Metabolism*. New York: Mary Ann Liebert; 1989: 7–14.

8. Han Z-H, Palnitkar S, Rao DS, Nelson D, Parfitt AM. Effect of ethnicity and age or menopause on the structure and geometry of iliac bone. *J Bone Miner Res.* 1996;11:1967–1975.
9. Harris ST, Watts NB, Genant HK, et al. Effects of risedronate treatment on vertebral and nonvertebral fractures in women with postmenopausal osteoporosis: a randomized, controlled trial. Vertebral Efficacy with Risedronate Therapy (VERT) Study Group. *JAMA.* 1999;282:1344–1352.
10. Eriksen EF, Melsen F, Sod E, Barton I, Chines A. Effects of long-term risedronate on bone quality and bone turnover in women with postmenopausal osteoporosis. *Bone.* 2002;31:620–625.
11. Ste-Marie L-G, Sod E, Johnson T, Chines A. Five years of treatment with risedronate and its effects on bone safety in women with postmenopausal osteoporosis. *Calcif Tissue Int.* 2004;75:469–476.
12. Compston JE, Vedi S, Stellon AJ. Inter-observer and intra-observer variation in bone histomorphometry. *Calcif Tissue Int.* 1986;38:67–70.
13. Power J, Loveridge N, Lyon A, Rushton N, Parker M, Reeve J. Bone remodeling at the endocortical surface of the human femoral neck: a mechanism for regional cortical thinning in cases of hip fracture. *J Bone Miner Res.* 2003;18:1775–1780.
14. Keshawaraz NM, Recker RB. Expansion of the medullary cavity at the expense of cortex in postmenopausal osteoporosis. *Metab Bone Dis Relat Res.* 1984;5:223–228.
15. Bousson V, Meunier A, Bergot C, et al. Distribution of intracortical porosity in human midfemoral cortex by age and gender. *J Bone Miner Res.* 2001;16:1308–1317.
16. Harlick RM, Shapiro LG. *Computer and Robot Vision.* Vol. 1 Reading, MA: Addison-Wesley; 1992.
17. Parfitt AM. The physiologic and clinical significance of bone histomorphometric data. In: Recker RR, ed. *Bone Histomorphometry: Techniques and Interpretation.* Boca Raton, FL: CRC Press; 1983: 143–223.
18. Martin RB, Burr DB. The microscopic structure of bone. In: *Structure, Function, and Adaptation of Compact Bone.* New York: Raven Press; 1989:18–56.
19. Brockstedt H, Kassem M, Eriksen EF, Mosekilde L, Melsen F. Age- and sex-related changes in iliac cortical bone mass and remodeling. *Bone.* 1993;14:681–691.
20. Barth RW, Williams JL, Kaplan FS. Osteon morphometry in females with femoral neck fractures. *Clin Orthop Relat Res.* 1992;283:178–186.
21. Parfitt AM. Osteonal and hemi-osteonal remodeling: the spatial and temporal framework for signal traffic in adult human bone. *J Cell Biochem.* 1994;55:273–286.
22. Qiu S, Fyhrie DP, Palnitkar S, Rao DS. Histomorphometric assessment of haversian canal and osteocyte lacunae in different-sized osteons in human rib. *Anat Rec A Discov Mol Cell Evol Biol.* 2003;272:520–525.
23. Broulik P, Kragstrup J, Moskilde L, Melsen F. Osteon cross-sectional size in the iliac crest: variation in normals and patients with osteoporosis, hyperparathyroidism, acromegaly, hypothyroidism and treated epilepsy. *Acta Pathol Microbiol Immunol Scand [A].* 1982;90:339–344.
24. Bell KL, Loveridge N, Jordan GR, Power J, Constant CR, Reeve J. A novel mechanism for induction of increased cortical porosity in cases of intracapsular hip fracture. *Bone* 2000;27:297–304.
25. The Mathworks, Inc. *Image Processing Toolbox for Use with Matlab: User's Guide.* Natick, MA: Mathworks Inc.; 2004.
26. Parfitt AM. Skeletal heterogeneity and the purposes of bone remodeling: implications for the understanding of osteoporosis. In: Marcus R, Feldman D, Kelsey J, eds. *Osteoporosis.* San Diego: Academic Press; 1996:315–339.
27. Mödder UI, Khosla S. Skeletal stem/osteoprogenitor cells: current concepts, alternate hypotheses, and relationship to the bone remodeling compartment. *J Cell Biochem.* 2008;103:393–400.
28. Yeni YN, Brown CU, Wang Z, Norman TL. The influence of bone morphology on fracture toughness of the human femur and tibia. *Bone.* 1997;21:453–459.
29. Martin RB, Boardman DL. The effects of collagen fiber orientation, porosity, density, and mineralization on bovine cortical bone bending properties. *J Biomech.* 1993;26:1047–1054.
30. Martin RB, Ishida J. The relative effects of collagen fiber orientation, porosity, density, and mineralization on bone strength. *J Biomech.* 1989;22:419–426.
31. Schaffler MB, Burr DB. Stiffness of compact bone: effects of porosity and density. *J Biomech.* 1988;21:13–16.
32. Delmas PD. Treatment of postmenopausal osteoporosis. *Lancet.* 2002;359: 2018–2026.
33. Lips P, Courpron P, Meunier PJ. Mean wall thickness of trabecular bone packets in the human iliac crest: changes with age. *Calcif Tissue Res.* 1978;26:13–17.
34. Croucher PI, Garrahan NJ, Mellish RWE, Compston JE. Age-related changes in resorption cavity characteristics in human trabecular bone. *Osteoporos Int.* 1991;1:257–261.
35. Power J, Loveridge N, Lyon A, Rushton N, Parker M, Reeve J. Osteoclastic cortical erosion as a determinant of subperiosteal osteoblastic bone formation in the femoral neck's response to BMU imbalance: effects of stance-related loading and hip fracture. *Osteoporos Int.* 2005;16:1049–1056.
36. Mayhew PM, Thomas CD, Clement JG, et al. Relation between age, femoral neck cortical stability, and hip fracture risk. *Lancet* 2005;366:129–135.